Sub-Coulomb proton absorption for isotopes of zirconium and molybdenum

D. S. Flynn, R. L. Hershberger, and F. Gabbard
University of Kentucky, Lexington, Kentucky 40506
(Received 20 June 1979)

Total (p,n) cross sections were measured with enriched targets of ^{92,94}Zr and ^{94,95,96,98}Mo, from each threshold energy to ~6.7 MeV. Proton strength functions were deduced and compared with those of neighboring nuclei. The strength functions were characterized by a minimum which was interpreted as a valley between the 3*s* and 3*p* single-particle resonances. Optical-model calculations were performed to fit the deduced strength functions. Systematic variations in the depths of the absorptive potentials were found as a function of mass in the manner suggested by Johnson *et al.*

[NUCLEAR REACTIONS ^{92,94}Zr ^{94,95,96,98}Mo(p,n) E_p=1.7–6.7 MeV; measured total $\sigma(E)$. Deduced proton strength functions. Optical-model analysis, deduced absorptive potential well depths.]

I. INTRODUCTION

It has been shown in recent years that single-particle resonances can be observed in proton-absorption excitation functions at sub-Coulomb energies.[1] This, plus the fact that the width of a single-particle resonance is largely determined by the absorptive potential, has made possible systematic studies of the absorptive potential in the $A=100$ region. Johnson *et al.*[2] have found that the strength of the absorptive potential changes dramatically as a function of A with a peak occurring near $A=103$.

Johnson *et al.* measured (p,n) cross sections for $89 \leq A \leq 130$. They estimated differences between the (p,n) and the proton-absorption cross sections with Hauser-Feshbach calculations and then obtained absorption cross sections from the measured (p,n) cross sections and the normally small calculated differences. Only two nuclides were studied below the peak at $A=103$ and for both, the resulting absorption cross sections were very dependent on details of the Hauser-Feshbach calculations.[3]

In the present work, the (p,n) cross sections for a series of zirconium and molybdenum isotopes were measured (Sec. II). Hauser-Feshbach-model calculations were performed to convert to absorption cross sections (Sec III), and the cross sections were fitted with Johnson's optical potential (Sec. IV). These nuclei are ideal in that (except for ^{94,96}Mo) the threshold energies are low and the resulting absorption cross sections are essentially equal to the (p,n) cross sections from a few hundred keV above threshold to all higher energies. The results are discussed in Sec. V.

II. EXPERIMENTAL METHODS AND UNCERTAINTIES

The University of Kentucky model CN Van de Graaff accelerator provided a beam of 1.7–6.7 MeV protons which penetrated 1 mg/cm^2 self-supporting foils of isotopically enriched zirconium and molybdenum (the ^{92}Zr foil was actually 0.5 mg/cm^2). In the (p,n) measurements the neutrons were detected with the Kentucky polyethylene-sphere detector.[4] In ancillary measurements to determine foil thicknesses, elastically scattered protons were observed with surface-barrier detectors. These experimental methods have been discussed elsewhere,[4-6] and only a discussion of the measurement uncertainties is presented here.

Three corrections were made to the (p,n) yields. Neutrons from sources other than the reaction of interest produced ~5% backgrounds at energies above the threshold; this was determined by counting with the beam passing through the target chamber with no target in place and by counting at energies less than the threshold energy. The targets were expected to be <99% atomically pure and from 94 to 98% isotopically pure. Small amounts of carbon, oxygen, and silicon were observed in elastic scattering spectra but estimated neutron yields from these impurities were insignificant. The experimental resolution was determined by the 30–60 keV energy loss the beam experiences in passing through the targets. The steeply rising cross sections and the experimental resolution combined to give energy average cross sections which were a few percent lower than the unaveraged cross sections. Corrections of 3–7% were made by parametrizing the cross sections' energy dependence with an $\exp(-\beta/E)$ form[1] and

calculating ratios of average to unaveraged cross sections. The third correction was for electronics dead time which caused a loss of ~1% of the pulses at the highest counting rates.

Except near threshold and at low energies where the cross sections are very small (<1 mb), the (p,n) cross sections were estimated to be accurate within ±7%. This value was obtained by adding the following uncertainties in quadrature: The target areal densities were uncertain to about ±5%, the efficiency of the spherical detector was known within ±3%, and the background subtraction introduced a cross section uncertainty of ~2%. The following possible sources of error were estimated each to contribute ≲1% to the cross section uncertainty: energy loss correction, counting statistics, beam energy uncertainty, beam integration, and dead time correction.

Beam energies were calibrated by measuring the ^{7}Li(p,n) and ^{27}Al(p,n) reactions over the threshold energies. Relativistic kinematic corrections were made. The energies were estimated to be accurate to ±0.1%.

Target areal densities were determined by counting back scattered protons at 2 MeV and using the Rutherford formula for the elastic scattering cross sections. Angular and energy dependences of the (p,p) yields were measured to be sure the Rutherford formula applied. At energies above 3 MeV the cross sections are known to deviate[7] from the Rutherford formula, but at 2 MeV the nuclear contribution to the back scattering cross sections is <1%. Resonances could cause the measured cross sections to deviate from the Rutherford formula: At 2 MeV the energy is below the threshold for isobaric analog resonances, the experimental resolution was too poor to observe resonances due to compound nucleus formation, and no resonances were observed. Multiple scattering of the protons affects the yields, especially when the angle between the detector and the target normal approaches ±90°, but this was not a problem above 1 MeV.

The elastic scattering yields were corrected for experimental resolution due to energy loss in the target (~3% correction) and dead time in the electronics (~2% correction). By precisely moving the target in the scattering chamber, the nonuniformity of each foil was determined and the uncertainty in the thickness experienced in the (p,n) measurement was estimated to be ~4%. This uncertainty was added in quadrature with those listed below to obtain the total thickness uncertainty of ±5%. Each of the following possible sources of error was estimated to contribute ≲1% to foil thickness uncertainties: target angle, energy loss correction, dead time correction, beam integration, beam energy, and counting statistics.

III. STRENGTH FUNCTIONS

The ^{98}Mo(p,n) excitation function is shown in Fig. 1. This is a typical example showing the exponentially rising cross section with some isobaric analog resonances at higher energies. Tables of cross sections for each of the measured reactions are available from the Physics Auxiliary Publication Service.[8]

The shapes of the (p,n) excitation functions are dominated by the exponential rise caused by the protons penetrating the Coulomb and centrifugal barriers. The barrier penetration factors can be calculated from Coulomb wave functions and, if the measurements are precise enough, one can divide out the barrier penetration effects and obtain experimental "reduced cross sections" or "l-wave averaged strength functions" which will reveal nuclear structure properties as the projectile energy and target mass are varied.[1,9,10]

Experimental strength functions were obtained from the relation

$$\mathrm{SF}(p,n) = R\,\frac{\sigma(p,n)}{4\pi^2 k^{-2}\sum_l (2l+1)P_l}\,,$$

where the P_l are the Coulomb penetration factors evaluated at the radius $R = 1.45A^{1/3}$ fm. Experimental (p,n) strength functions are shown in Figs. 2–7. In each case the transition from no (p,n) strength, below the threshold energy, to the average strength of ~0.3 fm occurs in an energy interval of ~0.5 MeV. The rapid rise occurs because of the large p-wave neutron transmission coeffi-

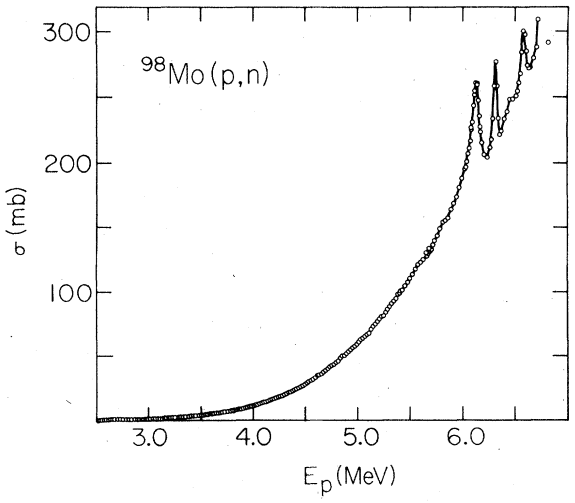

FIG. 1. Typical (p,n) excitation function showing the exponential rise due to barrier penetration effects.

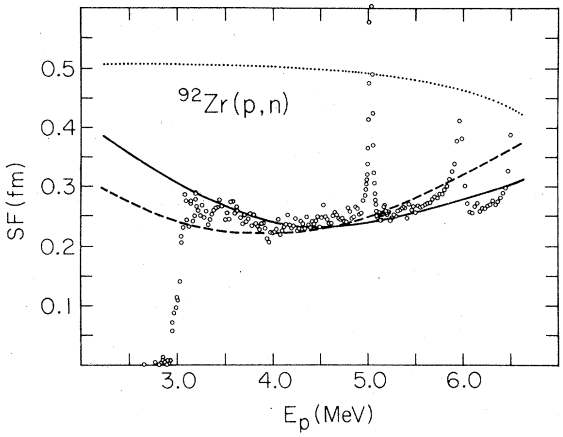

FIG. 2. $^{92}Zr(p,n)$ strength function. The solid curve represents the results of an optical-model fit. The dashed curve represents predictions made with Johnson's potential. The dotted line represents predictions obtained with the global potential of Becchetti and Greenlees (Ref. 12).

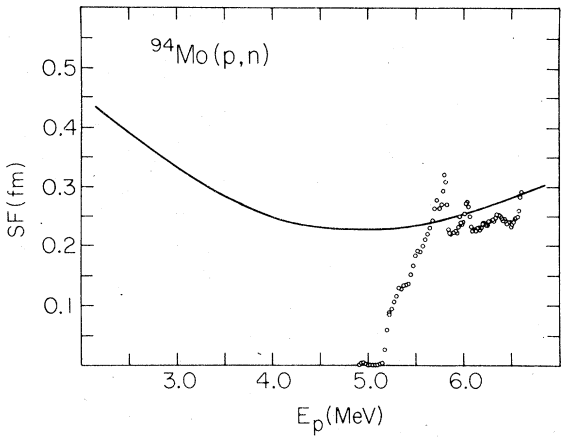

FIG. 4. $^{94}Mo(p,n)$ strength function. The solid curve represents the results of an optical-model fit.

cients in this mass region and because of the high level densities in the residual nuclei.

As a result the (p,n) strength function is essentially equal to the total proton strength function at energies greater than ~0.5 MeV above the threshold energies. Quantitative estimates of the (p,n)-to-absorption cross-section ratios were obtained by performing Hauser-Feshbach-model calculations. Many assumptions were made in these calculations, but since the obtained ratios were within 2% of unity above the threshold energies, errors in the calculation have a negligible effect on the optical-model analysis. The experimental (p,n) cross sections were multipled by the calculated absorption to (p,n) ratio and these "experimental" absorption cross sections were actually used in the optical-model fits described in the next section. Note that the calculated strength functions in Figs. 2–7 are total proton strength functions whereas the measurements shown are only (p,n) strength functions; they are not expected to be the same in the vicinity of, and below, the threshold energies.

IV. OPTICAL-MODEL CALCULATIONS

It has been suggested[2] that sub-Coulomb absorption cross sections in the mass 100 region can be described by a spherical optical potential whose absorptive well depth varies dramatically as a function of mass. The potential[1,2] is a conventional sum of Woods-Saxon, surface-absorptive, spin-

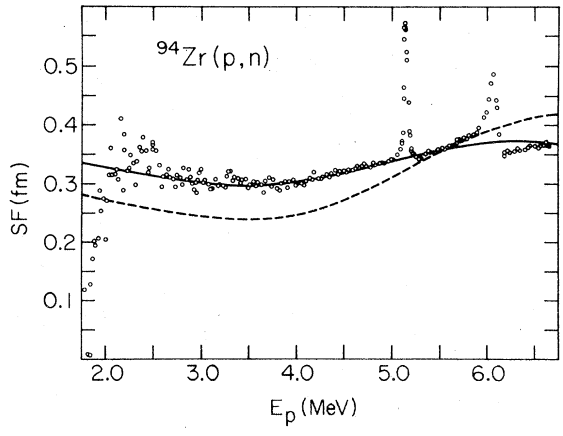

FIG. 3. $^{94}Zr(p,n)$ strength function. The solid curve represents the results of an optical-model fit. The dashed line represents predictions made with Johnson's potential.

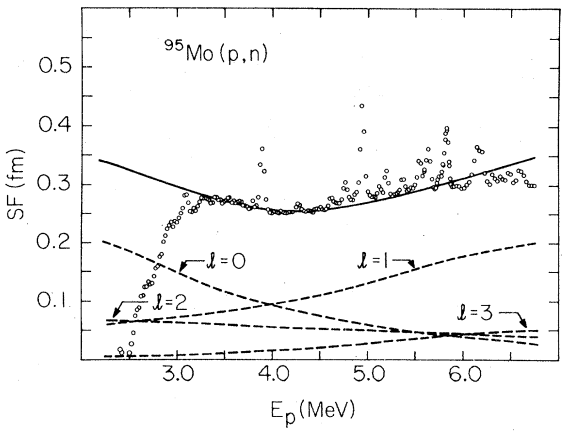

FIG. 5. $^{95}Mo(p,n)$ strength function. The dashed curves represent l-wave partial cross sections which contribute to make up the optical-model fit represented by the solid curve.

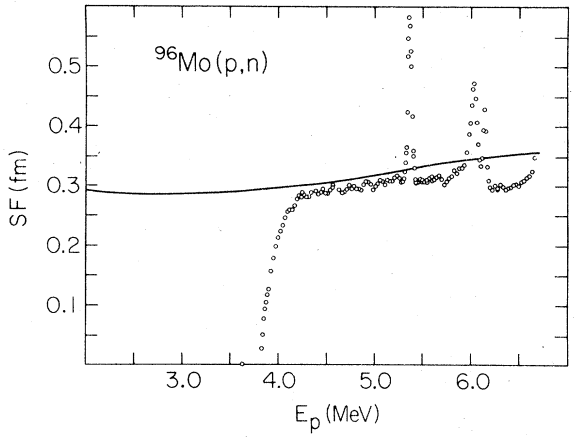

FIG. 6. ^{96}Mo(p,n) strength function. The solid curve represents the results of an optical-model fit.

orbit, and Coulomb potentials.[11]

Strength functions calculated with this potential are represented by the dashed curves in Figs. 2 and 3. [Real well depths were assumed to vary as $V_R(0) = V_0 + 24(N-Z)/A + 0.45Z/A^{1/3}$.] Differences between the predicted and experimental strength functions are evident but the shapes and magnitudes are in much better agreement than one obtains from the predictions of a global optical model: The dotted curve in Fig. 2 was obtained with the potential of Becchetti and Greenlees.[12]

Although fits to the measurements can be obtained with many different sets of potential parameters, there are some quantities that are quite well determined by the shape and magnitude of each strength function. Since structure in the strength function comes from various l waves resonating, the quantity VR^2 is determined by causing the maximum and minimum to occur at the correct energies. For example, the calculation for ^{92}Zr obtained with Johnson's potential can be seen in Fig. 2 (dashed curve) to have a minimum at 4 MeV. By reducing the real potential V_0 from 55.4 to 54.3 MeV, the minimum is shifted higher and a better fit is obtained (see the solid curve in Fig. 2). The curvature in the strength function is determined by the damping (spreading) of the resonances which occurs because of the absorptive potential. By adjusting the absorptive well depth W and the absorptive width a_D one can adjust the curvature and magnitude of the strength function. The values of these parameters are not unique and depend on the real potential geometry. However, from experience calculating and from Johnson's systematic studies[1] of χ^2 versus various parameters, it appears that the strength functions are most sensitive to variations in W and a_D. As an example of the effect of changing W and a_D, the dashed line in Fig. 3 was obtained with $W = 6.0$ MeV and $a_D = 0.4$ fm. Increasing W to 9.3 MeV and a_D to 0.42 fm damps the resonance and gives the fit represented by the solid line in Fig. 3.

Since angle integrated cross sections were measured, direct information about the partial l-wave cross sections was not obtained. The information can be inferred, however, by calculating the partial l-wave cross sections which make up one of the total cross section fits. An example is shown in Fig. 5. The broad minima seen in the ^{92,94}Zr and ^{95}Mo strength functions are seen to occur because of the s wave resonating at low energies and the p wave resonating at high energies.

In order to test Johnson's thesis that one can fit these strength functions by adjusting W as a function of A, fits to each individual strength function were obtained by searching on V_0 and W; data near the threshold energy and data near the isobaric analog resonances were omitted in the fitting procedure; a_D was fixed at 0.4 unless it was found that a much better fit could be obtained by changing it. The solid lines in Figs. 2–7 represent the cal-

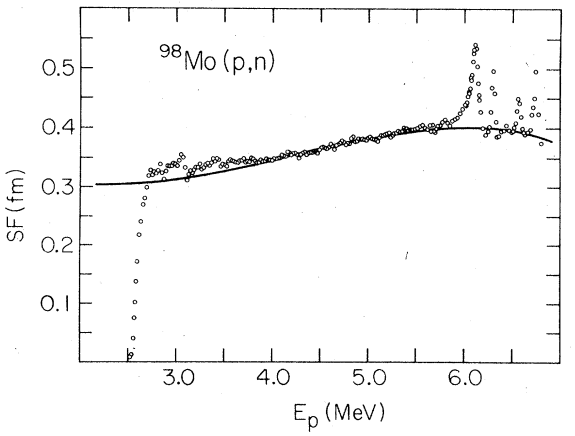

FIG. 7. ^{98}Mo(p,n) strength function. The solid curve represents the results of an optical-model fit.

TABLE I. Optical-model parameters.

Target	W (MeV)	a_D (fm)	V_0[a] (MeV)
^{92}Zr	5.5	0.40	54.3
^{94}Zr	9.4	0.42	53.8
^{94}Mo	5.3	0.40	54.4
^{95}Mo	7.1	0.40	54.5
^{96}Mo	14.0	0.36	53.9
^{98}Mo	13.3	0.44	55.3

[a] The real potential at zero energy $V_R(0)$ is related to V_0 by $V_R(0) = V_0 + 24(N-Z)/A + 0.45Z/A^{1/3}$.

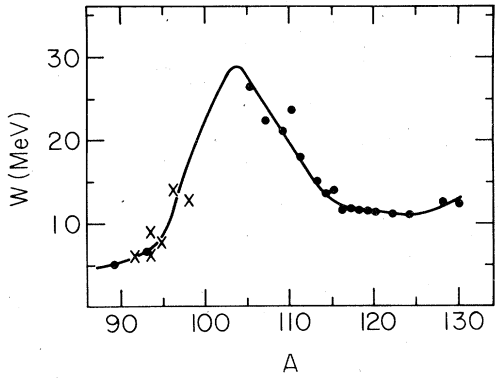

FIG. 8. Absorptive well depths versus mass number. The crosses represent the values obtained by fitting the measured cross sections. The solid dots and the curve represent the values of W and the visually drawn curve presented by Johnson *et al.* in Ref. 2.

culated fits. The corresponding parameters are listed in Table I. (So little of the ^{94}Mo and ^{96}Mo strength functions was obtained that it was hardly meaningful to try to fit them; the parameters listed for them in Table I are not unique and only serve to indicate one possible fit.) It is interesting to notice that the values of V_0 are ~1 MeV less than the 55.4 MeV expected from the analyses of the precision tin(p,n) cross sections.[1] Johnson *et al.*[3] also found it necessary to use V_0 approximately 54.4 MeV in order to fit the ^{89}Y(p,n) and ^{93}Nb(p,n) cross sections. V_0 is seen to be constant to within ±2%; the diffuseness a_D varies ±10%; but W ranges from 5.3 to 14 MeV. In Fig. 8 values of W versus A are plotted. The dots represent values reported by Johnson *et al.*; the crosses represent the values listed in Table I.

V. CONCLUSIONS

In spite of the steeply rising (p,n) excitation functions encountered at sub-Coulomb energies, measurements can be performed precisely enough to yield information about the nuclear structure. In the zirconium and molybdenum isotopes studied, the obtained spherical-optical-model parameters varied from one nuclide to the next; nevertheless, there is a clear trend for the absorptive well depth to increase with A in just the manner suggested by Johnson *et al.*[2]

It is expected that the absorptive potential should be significantly smaller near nucleon shell closures.[13,14] It is not clear, however, that the changes in the absorption should be characterized by varying the well depth W only; for example, Becchetti and Greenless[12] observed a mass dependence in the surface absorption, but then found that introducing a term proportional to $(N-Z)/A$ into the imaginary diffuseness a_D gave the most significant improvements to the fits. (Note, however, that their variations in a_D were only ~10% over the mass 100 region.) In the present experiment the differing shapes of the strength functions give rise to the different values of W; it was not possible to describe the strength functions by varying a_D instead of W. The single-particle resonances significantly affect the shapes of the strength function in these experiments, making it possible to resolve the W a_D ambiguity. Johnson *et al.*[1] demonstrated this in the tin isotopes by examining the χ^2 quality of fit while a_D was changed and V_0 and W were then searched on to obtain best fits: V_0 and W could not compensate for changes in a_D.

The real potential geometry affects the strength function also[1]; yet, in the present analysis it was assumed to vary only in a conventional way. There still remains a question of whether or not A dependent variations in the real geometry might change the anomalous A dependence of W. We are presently analyzing the results of elastic scattering measurements in hopes of better determining the real potential geometry applicable to these masses and energies.

ACKNOWLEDGMENTS

The authors wish to thank Dr. C. H. Johnson, Dr. R. Schrils, and Dr. M. T. McEllistrem for helpful discussions. Dr. C. Hagan and Dr. K. K. Sekharan helped with some of the data collection. This work was supported in part by a grant from the National Science Foundation.

[1]C. H. Johnson, J. K. Bair, C. M. Jones, S. K. Penny, and D. W. Smith, Phys. Rev. C 15, 196 (1977).
[2]C. H. Johnson, A. Galonsky, and R. L. Kernell, Phys. Rev. Lett. 39, 1604 (1977).
[3]C. H. Johnson, A. Galonsky, and R. L. Kernell (unpublished).
[4]K. K. Sekharan, H. Laumer, B. D. Kern, and F. Gabbard, Nucl. Instrum. Methods 133, 253 (1976).
[5]D. S. Flynn, K. K. Sekharan, B. A. Hiller, H. Laumer, J. L. Weil, and F. Gabbard, Phys. Rev. C 18, 1566 (1978).
[6]F. Gabbard, D. S. Flynn, and R. L. Hershberger, in Proceedings of the Fifth Conference on the Application of Small Accelerators, IEEE Trans. Nucl. Sci. NS26, 1212 (1979).
[7]Elastic scattering excitation functions of protons from ^{92,94}Ar and ^{94,95,96,98}Mo have been measured and are presently being analyzed and prepared for publication.

[8]See AIP document No. PAPS PRVCA 20-1700-6 for 15 pages of tables of cross sections. Order by PAPS number and journal reference from American Institute of Physics, Physics Auxiliary Publications Service, 335 East 45th Street, New York, New York 10017. The prices is $1.50 for microfiche or $5 for photocopies. Airmail additional. Make checks payable to the American Institute of Physics. This material also appears in *Current Physics Microfilm*, the monthly microfilm edition of the complete set of journals published by AIP, on frames immediately following this journal article.

[9]G. A. Jones, Nucl. Phys. 12, 167 (1958).

[10]A. J. Elwyn, A. Marinov, and J. P. Schiffer, Phys. Rev. 145, 957 (1966).

[11]Coulomb radii of $1.23A^{1/3}$ were taken from electron scattering results tabulated in R. C. Barrett and D. F. Johnson, *Nuclear Sizes and Structure* (Clarendon, Oxford, 1977), pp. 156–158.

[12]F. D. Becchetti, Jr. and G. W. Greenlees, Phys. Rev. 182, 1190 (1969).

[13]A. M. Lane, J. E. Lynn, E. Melkonian, and E. R. Rae, Phys. Rev. Lett. 2, 424 (1969).

[14]J. E. Lynn, *Theory of Neutron Resonance Reactions* (Clarendon, Oxford, 1968).